Experimental Cell Research **255,** 47–55 (2000)
doi:10.1006/excr.1999.4761, available online at http://www.idealibrary.com on IDEAL®

Expression of the Adenovirus Receptor and Its Interaction with the Fiber Knob

Richard P. Tomko,* Clas B. Johansson,† Maxim Totrov,* Ruben Abagyan,*
Jonas Frisén,† and Lennart Philipson*,†,[1]

*Skirball Institute of Biomolecular Medicine, New York University Medical Center, 550 First Avenue, New York, New York 10016; and
†Department of Cell and Molecular Biology, Karolinska Institute, Box 285, SE-17177 Stockholm, Sweden

The coxsackievirus group B (CVB) and adenovirus (Ad) receptor (HCVADR, formerly HCAR) is a cell surface protein with two immunoglobulin-like regions (IG1 and IG2) that serves as a receptor for two structurally unrelated viruses. We have established the tissue distribution of the receptor in the rodent by immunohistochemistry and show that the receptor is broadly expressed during embryonic development in the central and peripheral nervous systems and in several types of epithelial cells. The tissue distribution is more restricted in the adult but remains high mainly in epithelial cells. Using site-directed mutagenesis, based on computer modeling of the IG1 region, Ad5 binding could be inhibited but CVB attachment was unaffected. A double amino acid substitution in a three-stranded anti-parallel β sheet that may form a face of the receptor completely inhibited Ad5 binding. Therefore, we conclude that the molecular interactions critical for Ad5 binding to HCVADR do not overlap with those of CVB3. In fact a specific antibody interfering with only CVB binding recognizes the IG2 domain in the receptor, suggesting that the CVB interacts with this region or an overlap between the IG1 and the IG2 regions.

INTRODUCTION

The study of the human and mouse CVADR[2] (HCVADR and MCVADR, respectively) is of interest for two reasons: (i) understanding the role receptors play in the pathogenic process of both the CVB and the AdC and (ii) furthering the development of adenovirus-based gene therapies through awareness of receptor distribution and function.

The HCVADR and MCVADR are 46-kDa cell surface proteins whose isolation and characterization have been previously described [1–3]. Analysis of their amino acid sequences shows that they are greater than 80% identical and are distantly related to the immunoglobulin superfamily of proteins [1]. This classification is distinguished by a distinctive fold that results from a sandwich of two anti-parallel β sheets that are stabilized by hydrophobic interactions and a conserved disulfide bond [4]. The folded domains are classified as C domain or V domain based upon the composition and number of amino acids that separate the conserved cysteine residues. Members of this family, such as NCAM [5] and PDGFR [6], as well as MHC class I [7, 8] and II [9], participate in diverse cellular functions such as cell adhesion, growth factor receptor, and antigen presentation, respectively. Ligand interaction is not limited to a particular region of the IG domain since recognition can occur either through determinants on the β sheets or on loops between β strands [4].

IG-domain-containing molecules have already been identified as receptors for the picornaviruses [10–14]. The *Picornaviridae* are small unenveloped icosahedral viruses that contain four different capsid proteins, VP1, VP2, VP3, and VP4 [15]. In the mature virus, a single strand of RNA is surrounded by 60 copies of each capsid protein. The resolved crystal structure of the serotype 3 of CVB reveals that the VP1–VP3 molecules maintain a β sandwich structure conserved among picornaviruses [16]. The association of these molecules on the virus surface forms hydrophobic depressions around the fivefold and twofold axes of symmetry, generating potential sites for receptor binding. Since all six CVB serotypes compete for binding to the same receptor [17] and share the strongest conservation of amino acids within the fivefold depression [16], it may be the major region for receptor attachment. This canyon is capable of binding the cellular receptor [18] for the major group of human rhinoviruses (HRV).

In contrast to the *Picornaviridae,* little is known about adenovirus receptors beyond the existence of the recently isolated CVADR. A recent claim that the MHC class I heavy chain may serve as the receptor for AdC

[1] To whom reprint requests should be addressed at the Karolinska Institute, Box 285, SE-17177 Stockholm, Sweden. E-mail: Lennart.Philipson@cmb.ki.se.

[2] Abbreviations used: Ad, adenovirus; CVB, group B coxsackieviruses; HCAR and MCAR, human and mouse receptors for CVB and adeno2 and 5, correctly referred to as CVADR.

0014-4827/00 $35.00

has not yet been confirmed [19]. The *Adenoviridae* are substantially more complex, containing 11 structural proteins of which 7 comprise the capsid. The capsid surrounds a linear double-stranded DNA genome to form the mature particle [20]. Similar to the CVB, adenovirus is an icosahedron. However, adenoviruses contain antenna-like fiber molecules that protrude from the vertices and terminate in the globular carboxy-terminal knob structure [20]. Virus binding to cellular receptors takes place via the knob domain [21, 22], formed from the trimeric association of eight-stranded anti-parallel β-sandwich monomers [23]. The crystal structure of the Ad5 knob reveals a central depression centered on the threefold axis of symmetry and three symmetry-related valleys that result from the close association of knob monomers. Amino acids that line the central and valley depressions are conserved between members of the AdC (Ad2 and Ad5) competing for the same receptor, suggesting that these conserved residues are critical for virus–receptor interaction much like that for the CVB [23].

Although competition of the AdC and CVB for receptor binding was known, the recent isolation of the CVADR cDNAs [2, 1] allowed more detailed analysis of this interaction. We have developed a three-dimensional model of HCVADR using this structure in docking scenarios to define the sites of CVB and Ad5 attachment. The results demonstrate differential molecular interactions of CVB and Ad5 with HCVADR which are confirmed through targeted mutations of the receptor and through expression studies using different specific antibodies. The expression of the receptor protein during mouse embryogenesis and in adult tissues is also reported.

MATERIALS AND METHODS

Domain recognition. Amino acid sequences were characterized according to Needleman and Wunsch [24] comparisons with zero end-gap penalties performed with all the sequences in the SwissProt protein sequence database and Brookhaven database. Statistical significance of similarities was evaluated on the basis of 4 million comparisons between sequences of protein domains with known 3D structure (R. A. Abagyan and S. Batalov, manuscript in preparation).

Model building. We built a model of the first IG-like domain (IG1) of the extracellular part of the HCVADR and MCVADR on the basis of presumed sequence and structural similarity to the monoclonal antibody against cholera toxin peptide 3 (PDB code 1tet). It has a sequence identity of 28% over approximately 100 residues. The second IG-like domain, IG2 (residues 127–233), and the connection between IG1 and IG2 were built by homology with residues 89 to 178 of the T-cell surface glycoprotein CD4 (PDB code 3cd4). The sequence identity between the CD4 fragment and the 127–233 region of the receptor was 21%. The sequence of IG1 and IG2 domains was threaded onto 1tet and 3cd4, and the initial sequence alignment was adjusted to make it consistent with the immunoglobulin topology. The side chains were placed by global energy minimization [25].

Docking of the receptor. Docking of the 3D model of the CVB3 receptor to the canyon of the virus was performed on the basis of the low-resolution structure of the human rhinovirus with the ICAM1 receptor, as well as shape complementarity between the receptor model and the structure of the coxsackievirus (1cox). An analytical molecular surface was built with the contour-buildup algorithm [26] implemented in the ICM program. Docking solutions have been generated by the Brownian Monte Carlo procedure [25, 27].

Viruses. The Nancy strain of CVB3 was used for all experiments. ^{35}S-virus was prepared in HeLa cells grown in 150-cm^2 tissue culture flasks. Monolayer cultures were rinsed with 1× PBS and inoculated with 1 ml of undiluted crude virus (>10^8 PFU/ml). After 90 min at 37°C, with intervals of rocking to attain uniform attachment of virus to cells, cultures were overlaid with 9 ml of Met/Cys-deficient medium and incubated at 37°C for 2 h. The growth medium was decanted, and 9 ml of fresh growth medium containing 0.5 mCi of label (^{35}S Trans Label; ICN) was added. Flasks were incubated at 37°C overnight before the monolayers were alternately frozen and thawed three times to release intracellular virus. The resultant suspension was centrifuged for 10 min at 4000 rpm at 4°C to remove cellular debris. The supernatant fluids were brought to 1% sodium dodecyl sulfate (SDS) and the virus was pelleted through 10 ml of a cushion of 30% sucrose in 1× PBS with 0.5% bovine serum albumin at 24,000 rpm for 4 h at 18°C in an SW27 rotor. The supernatant fluids were decanted, and the virus pellets were resuspended at 4°C overnight in 2 ml of 10 mM NaCl, 10 mM Tris–HCl, 1 mM $MgCl_2$, pH 7.35. The following day, EDTA was added to a concentration of 2 mM and the resuspended pellets were centrifuged on a discontinuous CsCl gradient at 33,000 rpm for 4 h at 12°C in an SW40 rotor. The gradient was fractionated by collecting 500-μl fractions with a needle inserted at the bottom of the centrifuge tube. Each fraction was assayed for virus content by counting 1-μl samples in a scintillation counter. Fractions with significant counts were pooled and dialyzed against 1× PBS overnight.

Labeled Ad5 virus was prepared in 293 cells by the addition of 50 μCi/ml ^{35}S Trans Label (ICN) to growth medium containing reduced Met/Cys. Virus was purified as previously described [28] except that NP-40 was omitted from the lysis solution.

Mutants. The following mutants were constructed using the pRTHR plasmid (HCVADR Accession No. U90716) [1], the QuikChange mutagenesis kit (Stratagene), and the following oligonucleotides: ΔAD primer 1, 5′-AAGGTGGATCAAGCGATTGATTTATATTCTGGA-3′; ΔAD primer 2, 5′-TCCAGAATATAAATCAATCGCTTGATCCACCTT-3′; ΔCB1 primer 1, 5′-ACGAGTAATGATGCCGAGGAGGGTGATGCATCA-3′; ΔCB1 primer 2, 5′-TGATGCATCACCCTCCTCGGCATCATTACTCGT-3′; ΔCB2 primer 1, 5′-CTTAGTCCCGCAGACCAGGGA-3′; and ΔCB2 primer 2, 5′-TCCCTGGTCTGCGGGACTAAG-3′. Amplification was performed using a Perkin–Elmer 9600 thermal cycler for 18 alternating cycles of 95°C for 1 min and 68°C for 14 min. Wild-type plasmids were removed from the amplification reaction by digestion with *Dpn*I and the mutated plasmids concentrated by precipitation with 2 volumes of ethanol and 20 μg of glycogen following phenol–chloroform extraction. The precipitated DNA was resuspended in 10 μl of water of which 1 μl used to electroporate the *Escherichia coli* strain XL1-Blue.

The ΔCB mutants were constructed using pRTHR, the Transformer site-directed mutagenesis kit (Clontech), and the following oligonucleotides: Selection, 5′-CTTTTTTGGAAGCTTAGGCTTTTG-3′, and Mutation, 5′-CAAATTTACGCTGGATCCCGAAGAC-3′.

All plasmids were harvested using the alkaline lysis method and purified for transfection using CsCl gradient centrifugation [29].

Transfections. NIH3T3 cells were transfected using the Lipofectamine reagent (GIBCO). In brief, transfections were performed on varying scales with 7 μl of Lipofectamine and 2 μg of DNA per 6 × 10^5 cells. The lipid–DNA mixture was incubated with the cells for 5 h before being replaced with fresh DMEM containing 10% FCS. Transfectants were used in assays 24 h after the beginning of transfection.

Virus and Western blots. Transfectants were solubilized in 1% Triton X-100 and 1% deoxycholate. Recovered proteins were sepa-

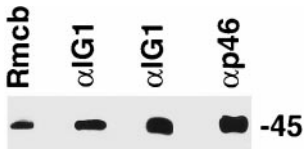

FIG. 1. A Western blot demonstrating the specificity of the IG1 rabbit antibody raised against the purified *E. coli* GST fusion protein. Cell extracts from HCAR-transformed NIH3T3 cells (lanes 3 and 4) or mouse brain (lane 2) were used and probed with the indicated antibodies. RcmB is a monoclonal against the HCVADR but only under nondenaturing conditions (lane 1), anti-p46 is a rabbit antibody against the MCVADR which obviously cross reacts with the human receptor. Anti-IG1 detects both the human and the mouse receptor.

rated by SDS–10%PAGE using the discontinuous buffer system with or without heating or addition of reducing agents [30]. Proteins were transferred from the gel to a PVDF support and probed with 1×10^6 cpm of ^{35}S-Ad5 or ^{35}S-CVB3N for 4 h at room temperature. The membranes were washed 3× for 15 min each in 50 ml of 1× PBS and exposed to autoradiographic film.

Filters for Western blots were prepared as above and probed with either 125 ng/ml Rcmb or a 1:500 dilution of anti-p46. Rabbit antibodies to GST fusion proteins containing either the IG1 or the IG1+IG2 domains of the receptor were also used. Primary antibody reactivity was visualized using a horseradish peroxidase-conjugated secondary antibody and the ECL Western Blotting Detection System (Amersham).

Immunohistochemistry. Cryostat sections from embryonic day 15 mouse embryos were rehydrated in PBS and endogenous peroxidase was quenched with 0.3% hydrogen peroxide in methanol. They were then rinsed in PBS; blocked in PBS with 0.2% BSA, 3% goat serum, and 0.05% Triton X100 for 30 min; incubated at 37°C for 120 min with rabbit anti-MCVADR antibody (αIG1 1:200); and rinsed in PBS followed by incubation with a biotinylated anti-rabbit antibody (1:300) for 45 min at 37°C and detection with Vectastain ABC kit with DAB according to the manufacturer's recommendation.

Cryostat sections from adult rat were incubated with the rabbit anti-MCVADR antibody (1:50) for 1 h at 37°C, rinsed in PBS, and incubated with a swine anti-rabbit FITC antibody (1:15) DAKO for 45 min at room temperature.

Labeling and viral infection of ependymal cells. Unilateral stereotaxic injections of 10^9 CMV-lacZ adenovirus plaque-forming units in 10 mM Tris–HCl were made into the lateral ventricle.

RESULTS

Receptor Expression

Antibodies produced in rabbits against the overproduced GST fusion protein containing the IG1 domain of the CNADR were compared with the monoclonal Rmcb and the anti-p46 antibody in Western blots (Fig. 1). The anti-IG1 recognized only a single protein in mouse brain extracts and the HCVADR overexpressed in NIH3T3 cells, both of the same molecular weight around 46 kDa (Fig. 1). In fact both the anti-p46 and the anti-IG1 recognized the Rmcb receptor in both mouse and man, but the monoclonal only identified the HCVADR under nondenaturing conditions.

Serially sectioned embryonic day 15 mouse embryos were used to establish the organ distribution of the receptor by immunohistochemistry. Figure 2 demonstrates that the receptor is abundant in epithelial cells in several organs. The basal cell layer in the skin and the epithelia in the intestine, mouth, and nose showed strong labeling (Fig. 2 and data not shown). MCVADR immunoreactivity was abundant throughout the developing central nervous system and in peripheral nerves at this developmental stage. In adult tissues the expression was more restricted. In the adult rodent brain, labeling was largely limited to ependymal cells lining the ventricular system (Fig. 3). After adenovirus injection into the lateral ventricle of adult rats with replication-deficient adenovirus expressing *lacZ* under control of the CMV promoter, reporter gene expression was confined to ependymal cells (Fig. 3A). The ependymal cells showed immunoreactivity for the adenovirus receptor predominantly on their apical side (Fig. 3B). In the adult respiratory system, MCVADR immunoreactivity was strong in the apical membrane of epithelial cells in the trachea and bronchi, but undetectable in the alveoli of the lung (Fig. 4). In several other tissues, including kidney, liver, and intestine, epithelial cells expressed the receptor (Fig. 4). Scattered MCVADR-immunoreactive cells were also seen in pancreas and heart (Fig. 4).

Structural Elements and Model Construction

Direct sequence comparison of the extracellular fragment of CVADR with proteins of known 3D structure showed significant similarity with heavy chains of immunoglobulin FAB fragments (PDB codes 1neu, 1tet, 1iai, 1dbb, 1ggi, 1mco, 7fab, etc.). The heavy chain of anti-cholera toxin (1tet) aligns with 27% sequence identity. Therefore we conclude that two immunoglobulin-like domains, referred to as IG1 and IG2, form the extracellular part of the receptor.

The cytoplasmic domain was found to be similar to several Ser-Pro-Thr-rich domains in the TFG protein related to the papillary thyroid carcinoma and p68 TRK-T3 oncoprotein. No related proteins with known function or 3D structure were found. In the beginning of the cytoplasmic domain a sequence fragment, RKKRREEKY, matches two possible signatures for a tyrosine kinase phosphorylation site ([RK]-x-x-[DE]-x-x-x-Y or [RK]-x-x-x-[DE]-x-x-Y). Tyrosine 269, therefore, may be involved in signal transduction via tyrosine phosphorylation and dephosphorylation as suggested [2]. Three other tyrosines do not have the required upstream sequence pattern and are less likely, although still possible, candidates for signal transduction.

To build a 3D model, we used homology to the heavy chain of an antibody (1tet) with known 3D structure to shape IG1 and homology with CD4 (3cd4) to build the

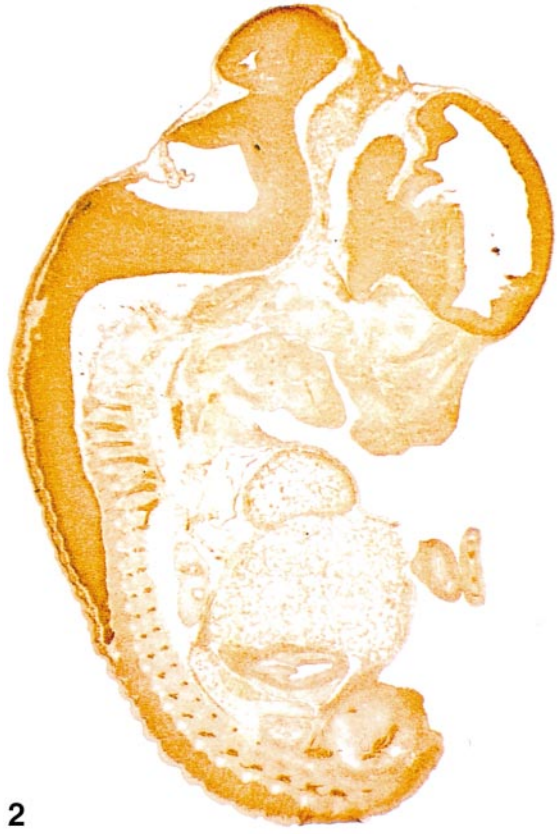

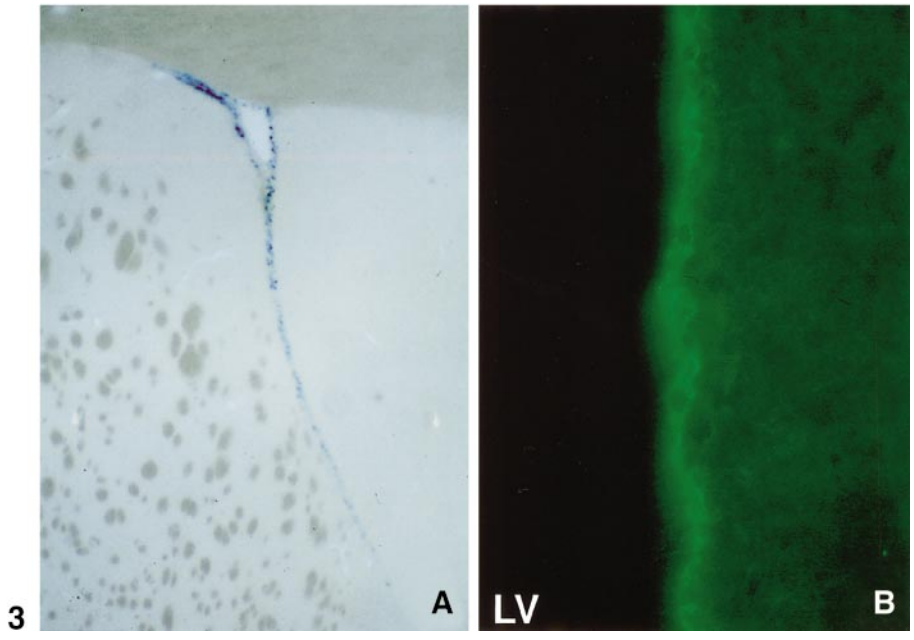

FIG. 2. Immunohistochemical localization of the MCVADR adenovirus receptor in a day 15 mouse embryo. Strong immunoreactivity is seen in the central nervous system, in dorsal root ganglia, and in peripheral nerves, as well as in epithelial cells in several organs.

FIG. 3. Distribution of the adenovirus receptor in the adult central nervous system. Ependymal cells lining the lateral ventricle express β-galactosidase after infection with a CMV-lacZ adenovirus (A). MCVADR immunoreactivity is restricted to ependymal cells in the wall of the lateral ventricle (B).

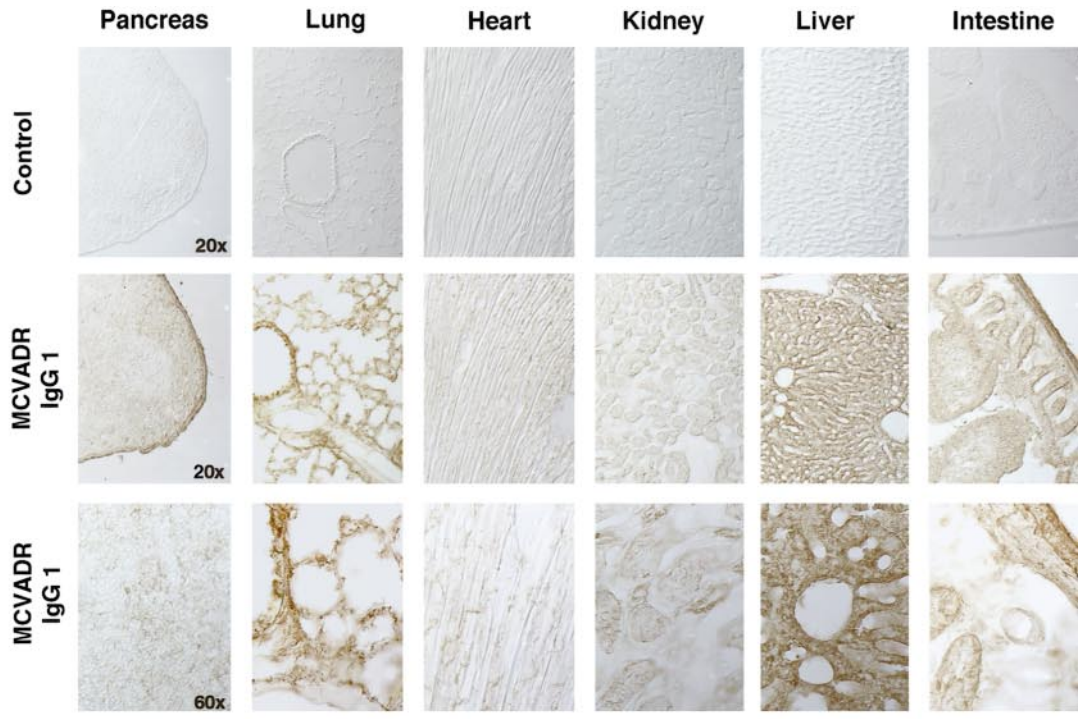
Pancreas
Lung
Heart
Kidney
Liver
Intestine
Control
MCVADR IgG 1
MCVADR IgG 1
20x
20x
60x

4

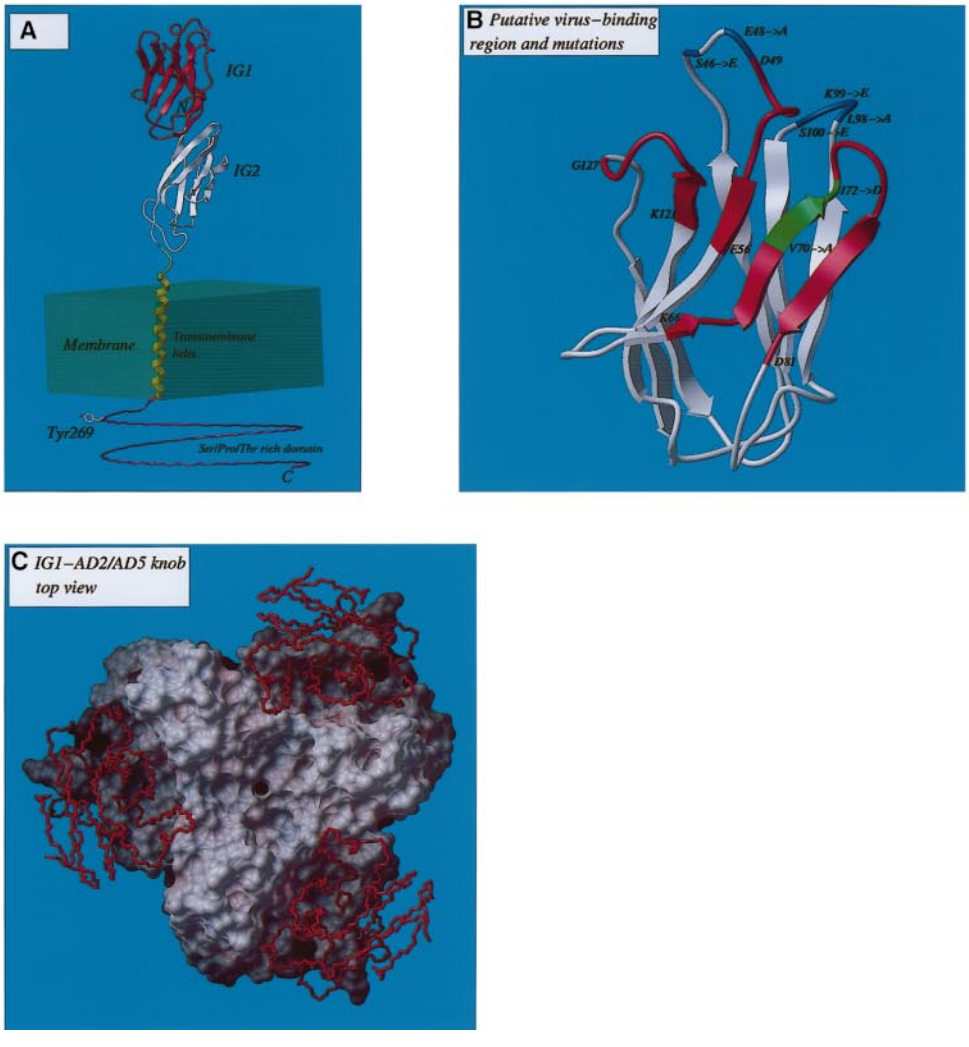
A
IG1
IG2
Membrane
Transmembrane helix
Tyr269
Ser/Pro/Thr rich domain
B Putative virus–binding region and mutations
E48->A
S46->E
D49
K99->E
L98->A
S100->E
G127
I172->D
K128
E56
V70->A
K66
D81
C IG1–AD2/AD5 knob top view

5

rest of the extracellular domain. The ICM program (Molsoft) was used to thread the receptor sequence onto its 3D template and energy minimize the model (Figs. 5A and 5B).

Receptor–Coxsackievirus Interaction

The CVB3 structure was recently solved to 3.5 Å resolution [16]. They predicted that the primary receptor-binding site on CVB3 is the canyon formed around the fivefold axis of icosahedral picornaviruses. Cryo-electron microscopy of another picornavirus, a human rhinovirus, with its receptor ICAM-1 [18], showed that the monomeric N-terminal IG domain D1 of ICAM-1 contains the primary binding site which interacts with the canyon of HRV16. Two IG amino-terminal domains of the CD4 receptor of HIV1, for which the structure has been determined at atomic resolution [31], were used instead of the ICAM-1 subunit to reconstruct the HRV14–ICAM-1 complex at 28 Å resolution [18] and confirm the proposed binding of the tip of the first IG domain of the receptor to the canyon.

We analyzed the molecular surface and electrostatic potential of the canyon in the 3.5-å resolution structure of CVB3 and performed docking of the HCVADR model to the canyon. The tip of the IG1 domain of the HCVADR model may fit into the canyon and, therefore, mimic the fit of the D1 domain of ICAM-1 into the canyon of the rhinovirus.

Receptor–Adenovirus Interaction

Xia *et al.* [23] solved the structure of the carboxy-terminal knob domain of the adenovirus type 5 fiber at 1.7 å resolution and suggested that both the central surface depression surrounding the threefold axis (Fig. 1C) and the side valleys are conserved and are candidates for binding sites for the cellular receptor.

We analyzed the surface of the trimer and concluded that the central surface depression around the threefold axis is not a favorable binding site for the IG1 domain of the receptor as recently proposed [32]. In contrast, the IG1 domain fits well to the side valley of the trimer. It forms an extended interaction interface in such a way that two β sheets of the knob and two β sheets of the receptor form a sandwich of four sheets. According to the proposed model (Fig. 5C), three receptor molecules can fit simultaneously on a single knob without steric hindrance.

TABLE 1

Amino Acid Substitutions of HCVADR

Mutants	HCVADR sequence	Mutant sequence
ΔAD	^{69}QVIIL^{73}	^{69}Q**A**I**D**L^{73}
ΔCB1	^{97}DLKSG^{101}	^{97}D**AEE**G^{101}
ΔCB2	^{47}PEDQG^{51}	^{47}P**A**DQG^{51}
ΔCB3	^{43}FTLSP^{47}	^{43}FTL**E**P^{47}

Note. Superscript numbers note the position of the first or last amino acid of the sequence. Sequences listed are linear as they appear in the HCVADR primary amino acid sequence. Substituted residues are in bold and underlined.

Mutational Analysis of HCVADR

Single or multiple amino acid substitutions were made in the N-terminal IG1 of HCVADR to determine the validity of the proposed receptor–virus interactions (Table 1). To assay the functionality of the mutant receptors, proteins were solubilized from transfected NIH3T3 cells and transferred to a polyvinyl transfer filter following separation by SDS–PAGE. Both ΔAd and ΔCB1 are expressed in transfected cells as they are visible on a Western blot using the HCVADR-specific monoclonal antibody Rcmb [33 and data not shown]. If the proposed binding of HCVADR within the canyon of CVB3 and along the valleys of the Ad5 knob is true, mutations in the respective binding areas should eliminate virus attachment. As expected, ^{35}S-Ad5 could bind ΔCB1 while the double substitution in ΔAD eliminated ^{35}S-Ad5 attachment (Fig. 6). Neither ΔCB1 or subsequent mutants ΔCB2 and ΔCB3 inhibited the ability of ^{35}S-CVB3 and ^{35}S-Ad5 to bind receptors (Fig. 6 and data not shown).

However, we independently expressed either IG1 or IG1+IG2 as glutathione *S*-transferase fusion proteins in *E. coli* and probed a Western blot of the purified proteins with the anti-p46 antiserum [39]. Interestingly, anti-p46 is capable of blocking CVB infection, but only the IG1+IG2 fusion protein was recognized by the antiserum (Fig. 7). These results suggest that the

FIG. 4. Immunoperoxidase analysis of adenovirus receptor MCVADR localization in various adult rat tissues. The upper row shows control sections that were processed parallel to the adjacent sections in the middle row, but with the primary antibody omitted. No background staining could be detected. The middle visualizes the expression of the adenovirus receptor MCVADR in special tissue classes of epithelial cells. The bottom shows the same sections in a higher magnification.

FIG. 5. (A) A 3D model of the human and mouse CVADR. The IG1 and IG2 domains were built by homology with an immunoglobulin and the CD4 protein. The C-terminal SPT domain was assigned an arbitrary conformation. The Y269 is a potential phosphorylation site. (B) The N-terminal IG1 domain of the CVADR. The blue regions may interact with the canyon in the CVB structure and the red regions can interact with the adenovirus fiber knob. The green area shows the mutant preventing adenovirus attachment. All the mutants described in Table 1 are shown. (C) A docking model of the adenovirus fiber knob interacting with three IG1 receptor domains.

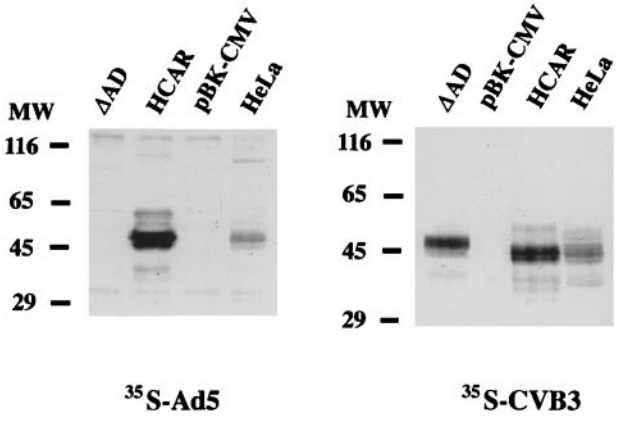

FIG. 6. A Western blot of ^{35}S-labeled virus attaching to mutant (ΔAD), wild-type (HCAR), and vector (pBK-CMV)-transformed cell extracts from NIH3T3 cells. A HeLa cell extract is included as a control.

molecular interactions necessary for stable binding of CVB to HCVADR may reside in the IG2 domain or the interface between the IG1 and the IG2 domains.

DISCUSSION

Here we present the tissue distribution of CVADR in the rodent and show a three-dimensional representation of the first interaction of the adenovirus with the host cell. Building upon the data from the solved crystal structures of the CVB3 and the Ad5 fiber knob, we show that the viruses may have distinct interactions with HCVADR, and for Ad5, the most critical area is localized to the β sheet forming one face of the receptor.

The tissue distribution of CVADR may indicate which cells can be infected by adenovirus and coxsackievirus group B. This is supported by the finding that adenovirus injection into the lateral ventricle of the brain resulted in infection of only ependymal cells, the only cell type close to the ventricle expressing CVADR (Fig. 3). Viral vectors may be valuable for introducing genes into cells of patients with distinct genetic disorders. Adenovirus is one of the more promising and intensively studied viruses for gene therapy. The reported tissue distribution of HCAVDR may serve as a guide to which cell types may be infected by adenovirus and may be helpful when selecting viral vectors for gene therapy.

In the field of picornavirus receptors the work has centered on the major group of HRV and their receptor human ICAM-1 [10, 13, 14]. ICAM-1 consists of five Ig-like domains (D1–D5) and serves as a receptor for fibrinogen, the integrins LFA-1 [34] and Mac-1 [35], and two pathogens in addition to HRV [36]. All of these various ligands except for Mac-1 bind to the most N-terminal D1 loop of ICAM-1 [36]. Mutational analysis [37] and structural studies [36, 18] confirm that the D1 loop is the site responsible for HRV binding. This binding takes place within the canyon structures of HRV that surround the fivefold axes of symmetry [18]. Since the CVB contain similar surface depressions it is believed that they are the sites of CVADR binding [16]. The electrostatic potential of the canyon detailed in the structure of the CVB provides a favorable environment for the interaction of the top of IG1 with CVB and we assumed that this interaction is similar to the D1 domain of ICAM-1 with HRV [18, 36].

Single amino acid substitutions within the BC or FG loops of ICAM-1 significantly inhibited the binding of HRV [37]. The fact that mutations within a single area did not exert a major influence over the binding of CVB3 to HCVADR is interesting but analogous with previous observations. Of the multitude of mutations made within D1 of ICAM-1 few had significant effects on the binding of various HRV serotypes [13, 37, 38]. Our results may be due to the nature of our selected substitutions or the fact that a comprehensive set of mutations was not generated across the loops of IG1. However, it is feasible that the large number of interactions between virus and receptor make it impossible to mutate a single structural motif of IG1 and disrupt virus binding. Perhaps there may also be a contribution from the second IG-like domain. Indeed, our results show that an antiserum that can protect cells against CVB infection [39] recognizes only the second domain of CVADR (Fig. 7). Thus antibody binding to IG2 may obstruct CVB attachment, but it is also conceivable that the tip of IG1 binds within the canyon and additional interactions stabilizing the virus–receptor complex occur between IG2 and surface regions of the capsid. It is also possible that the loop structures at the opposite end of the IG1 are the primary site of interaction.

In contrast, the studies with Ad5 do not show a contribution from IG2. Mutation of residues V70 and I72 completely abolished binding of Ad5 to isolated ΔAd receptor (Table 1). We also tested the ΔAd construct in a cell-based assay by staining for β-gal activity following incubation of transfectants with an Ad5 β-gal vector and found a decrease in cell staining of greater than 95% compared to controls (not shown).

FIG. 7. A Western blot of IG1 or IG1+IG2 GST fusion proteins produced in *E. coli* probed with the anti-p46 rabbit antibody preventing attachment of CVB3.

However, ΔAd appears to be at least very close to its native conformation since it retained the ability to bind CVB3 (Fig. 6) and the conformation-specific monoclonal antibody Rcmb [33] (not shown). In addition, this work defines the site of fiber attachment to the three valleys that encircle the fiber knob rather than the central depression. This may advance the design of small molecule inhibitors that fit into the valley and block attachment.

Studies of the events that govern internalization of the CVB and Ad are in the early stages. Little is known about CVB virus entry beyond receptor binding. But for Ad, the cellular attachment process appears to be a cooperative event between the fiber and the other capsid proteins, most notably the penton base [40]. A previous study showed that subgroup C Ad2 and subgroup D Ad9 both competed for the same cellular receptor, but Ad9 could infect cells in the presence of blocking amounts of competing fiber and the binding was facilitated by $\alpha_{v\beta}$ integrins [41]. The integrins do not bind to Ad fibers but rather to an RGD sequence located in the penton base proteins of most adenoviruses [41]. However, the RGD sequence is not present in all Ad serotypes, demonstrating that $\alpha_{v\beta}$ integrins are not a universal requirement [42]. More recently, it has been shown that serotypes from Ad subgroups A, C, D, E, and F all can bind to HCVADR through their fibers [43]. The report also hypothesized that cooperative binding between CVADR and $\alpha_{v\beta}$ integrins differs for the Ad serotypes. The length of the Ad fiber may influence the extent to which the viruses use a combination of CVADR and $\alpha_{v\beta}$ integrins for primary binding. Our results identify the site in CVADR that when altered or blocked may inhibit fiber binding of all Ad serotypes except subgroup B. This will facilitate studies of adenovirus penetration as to whether Ad uptake can occur exclusively through CVADR or what additional molecules may be involved in the uptake of the various Ad serotypes and what if any downstream signaling events occur following Ad binding to CVADR. The specific site for interaction may also be taken advantage of for introducing truncated forms of the receptor in cells not expressing the receptor [44] and thereby facilitating adenovirus gene therapy in resistant cells.

Note added in proof. The proposed attachment site of the receptor IG 1 domain on the fiber knob has been confirmed, verified and established through 2 papers recently published in *Science* (**286,** 1568–1570 and 1579–1582, 1999). Both these papers appeared after this communication was submitted and accepted.

The first paper demonstrated through mutational analyses that the AB-loop located in the side valley of the fiber knob is the attachment site for the receptor. The second paper demonstrated by crystallographic analyses of an ad 12 fiber knob-IG 1 domain complex that 3 receptor IG 1 domains can attach at the side valleys between the fiber knob monomers.

REFERENCES

1. Tomko, R. P., Xu, R., and Philipson, L. (1997). HCAR and MCAR: The human and mouse cellular receptors for subgroup C adenoviruses and group B coxsackieviruses. *Proc. Natl. Acad. Sci. USA* **94,** 3352–3356.
2. Bergelson, J. M., Cunningham, J. A., Droguett, G., Kurt-Jones, E. A., Krithivas, A., Hong, J. S., Horwitz, M. S., Crowell, R. L., and Finberg, R. W. (1997). Isolation of a common receptor for coxsackie B viruses and adenoviruses 2 and 5. *Science* **275,** 1320–1323.
3. Carson, S. D., Chapman, N. N., and Tracy, S. M. (1997). Purification of the putative coxsackievirus B receptor from HeLa cells. *Biochem. Biophys. Res. Commun.* **233,** 325–328.
4. Williams, A. F., and Barclay, A. N. (1988). The immunoglobulin superfamily—Domains for cell surface recognition. *Annu. Rev. Immunol.* **6,** 381–405.
5. Cunningham, B. A., Hemperly, J. J., Murray, B. A., Prediger, E. A., Brackenbury, R., and Edelman, G. M. (1987). Neural cell adhesion molecule: Structure, immunoglobulin-like domains, cell surface modulation, and alternative RNA splicing. *Science* **236,** 799–806.
6. Yarden, Y., Escobedo, J. A., Kuang, W. J., Yang-Feng, T. L., Daniel, T. O., Tremble, P. M., Chen, E. Y., Ando, M. E., Harkins, R. N., and Francke, U. (1986). Structure of the receptor for platelet-derived growth factor helps define a family of closely related growth factor receptors. *Nature* **323,** 226–232.
7. Becker, J. W., and Reeke, G. N., Jr. (1985). Three-dimensional structure of beta 2-microglobulin. *Proc. Natl. Acad. Sci. USA* **82,** 4225–4229.
8. Orr, H. T., Lancet, D., Robb, R. J., Lopez de Castro, J. A., and Strominger, J. L. (1979). The heavy chain of human histocompatibility antigen HLA-B7 contains an immunoglobulin-like region. *Nature* **282,** 266–270.
9. Kaufman, J. F., Auffray, C., Korman, A. J., Shackelford, D. A., and Strominger, J. (1984). The class II molecules of the human and murine major histocompatibility complex. *Cell* **36,** 1–13.
10. Greve, J. M., Davis, G., Meyer, A. M., Forte, C. P., Yost, S. C., Marlor, C. W., Kamarck, M. E., and McClelland, A. (1989). The major human rhinovirus receptor is ICAM-1. *Cell* **56,** 839–847.
11. Huber, S. A. (1994). VCAM-1 is a receptor for encephalomyocarditis virus on murine vascular endothelial cells. *J. Virol.* **68,** 3453–3458.
12. Mendelsohn, C. L., Wimmer, E., and Racaniello, V. R. (1989). Cellular receptor for poliovirus: Molecular cloning, nucleotide sequence, and expression of a new member of the immunoglobulin superfamily. *Cell* **56,** 855–865.

13a. Staunton, D. E., Merluzzi, V. J., Rothlein, R., Barton, R., Marlin, S. D., and Springer, T. A. (1989). A cell adhesion molecule, ICAM-1, is the major surface receptor for rhinoviruses. *Cell* **56,** 849–853.

13b. Staunton, D. E., Dustin, M. L., Erickson, H. P., and Springer, T. A. (1990). The arrangement of the immunoglobulin-like domains of ICAM-1 and the binding sites for LFA-1 and rhinovirus. *Cell* **61,** 243–254. [Published errata appear in *Cell,* 1990, **61,** 1157 and *Cell,* 1991, **66,** following 1311.]

14. Tomassini, J. E., and Colonno, R. J. (1986). Isolation of a receptor protein involved in attachment of human rhinoviruses. *J. Virol.* **58,** 290–295.
15. Rueckert (1990). *In* "Fields Virology" (B. N. Fields, D. M. Knipe, R. M. Chanock, M. S. Hirsch, J. L. Melnick, and J. P. Monath, Eds.), pp. 507–548, Raven Press, New York.
16. Muckelbauer, J. K., Kremer, M., Minor, I., Diana, G., Dutko, F. J., Groarke, J., Pevear, D. C., and Rossmann, M. G. (1995).

The structure of coxsackievirus B3 at 3.5 A resolution. *Structure* **3,** 653–667.

17. Crowell, R. L. (1976). Comparative genetic characteristics of picornavirus–receptor interactions. *In* "Ninth Miles International Symposium: Cell Membrane Receptors for Viruses, Antigens and Antibodies, Polypeptide Hormones and Small Molecules" (R. F. Beers and E. G. Bassett, Eds.), pp. 172–202, Raven Press, New York.
18. Olson, N. H., Kolatkar, P. R., Oliveira, M. A., Cheng, R. H., Greve, J. M., McClelland, A., Baker, T. S., and Rossmann, M. G. (1993). Structure of a human rhinovirus complexed with its receptor molecule. *Proc. Natl. Acad. Sci. USA* **90,** 507–511.
19. Hong, S. S., Karayan, L., Tournier, J., Curiel, D. T., and Boulanger, P. A. (1997). Adenovirus type 5 fiber knob binds to MHC class I alpha 2 domain at the surface of human epithelial and B lymphoblastoid cells. *EMBO J.* **16,** 2294–2306.
20. Stewart, P. L., Burnett, R. M., Cyrklaff, M., and Fuller, S. D. (1991). Image reconstruction reveals the complex molecular organization of adenovirus. *Cell* **67,** 145–154.
21. Louis, N., Fender, P., Barge, A., Kitts, P., and Chrobroczek, J. (1994). Cell-binding domain of adenovirus serotype 2 fiber. *J. Virol.* **68,** 4104–4106.
22. Henry, L., Xia, D., Wilke, E., Deisenhofer, J., and Gerard, R. D. (1994). Characterization of the knob domain of the adenovirus type 5 fiber protein expressed in E. coli. *J. Virol.* **68,** 5239–5246.
23. Xia, D., Henry, L. J., Gerard, R. D., and Deisenhofer, J. (1994). Crystal structure of the receptor-binding domain of adenovirus type 5 fiber protein at 1.7 A resolution. *Structure* **2,** 1259–1270.
24. Needleman, S. B., and Wunsch, C. D. (1970). A general method applicable to the search for similarities in the amino acid sequence of two proteins. *J. Mol. Biol.* **48,** 443–453.
25. Abagyan, R. A., Totrov, M. M., and Kuznetsov, D. N. (1994). ICM—A new method for protein modelling and design: Applications to docking and structure prediction from the distorted native conformation. *J. Comp. Chem.* **15,** 488–506.
26. Totrov, M., and Abagyan, R. (1996). The contour-buildup algorithm to calculate the analytical molecular surface. *J. Struct. Biol.* **116,** 138–143.
27. Totrov, M., and Abagyan, R. (1994). Detailed ab initio prediction of lysozyme–antibody complex with 1.6 A accuracy. *Nat. Struct. Biol.* **1,** 259–263.
28. Everitt, E., Sundquist, B., and Philipson, L. (1971). Mechanism of the arginine requirement for adenovirus synthesis. I. Synthesis of structural proteins. *J. Virol.* **8,** 742–753.
29. Sambrook, J., Fritsch, E. F., and Maniatis, T. (1989). "Molecular Cloning: A Laboratory Manual, Cold Spring Harbor Laboratory Press, Plainview, NY.
30. Laemmli, U. K. (1970). Cleavage of structural proteins during the assembly of the head of bacteriophage T4. *Nature* **227,** 680–685.
31. Ryu, S. E., Kwong, P. D., Truneh, A., Porter, T. G., Arthos, J., Rosenberg, M., Dai, X. P., Xuong, N. H., Axel, R., and Sweet, R. W. (1990). Crystal structure of an HIV-binding recombinant fragment of human CD4 [see comments]. *Nature* **348,** 419–426.
32. Freimuth, P., Springer, K., Berard, C., Hainfeld, J., Bewley, M., and Flanagan, J. (1999). Coxsackievirus and adenovirus receptor amino-terminal immunoglobulin V-related domain binds adenovirus type 2 and fiber knob from adenovirus type 12. *J. Virol.* **73,** 1392–1398.
33. Hsu, K. H., Lonberg-Holm, K., Alstein, B., and Crowell, R. L. (1988). A monoclonal antibody specific for the cellular receptor for the group B coxsackieviruses. *J. Virol.* **62,** 1647–1652.
34. Marlin, S. D., and Springer, T. A. (1987). Purified intercellular adhesion molecule-1 (ICAM-1) is a ligand for lymphocyte function-associated antigen 1 (LFA-1). *Cell* **51,** 813–819.
35. Diamond, M. S., Garcia-Aguilar, J., Bickford, J. K., Corbi, A. L., and Springer, T. A. (1993). The I domain is a major recognition site on the leukocyte integrin Mac-1 (CD11b/CD18) for four distinct adhesion ligands. *J. Cell Biol.* **120,** 1031–1043.
36. Bella, J., Kolatkar, P. R., Marlor, C. W., Greve, J. M., and Rossmann, M. G. (1998). The structure of the two amino-terminal domains of human ICAM-1 suggests how it functions as a rhinovirus receptor and as an LFA-1 integrin ligand. *Proc. Natl. Acad. Sci. USA* **95,** 4140–4145.
37. Register, R. B., Uncapher, C. R., Naylor, A. M., Lineberger, D. W., and Colonno, R. J. (1991). Human–murine chimeras of ICAM-1 identify amino acid residues critical for rhinovirus and antibody binding. *J. Virol.* **65,** 6589–6596.
38. McClelland, A., deBear, J., Yost, S. C., Meyer, A. M., Marlor, C. W., and Greve, J. M. (1991). Identification of monoclonal antibody epitopes and critical residues for rhinovirus binding in domain 1 of intercellular adhesion molecule 1. *Proc. Natl. Acad. Sci. USA* **88,** 7993–7997.
39. Xu, R., Mohanty, J. G., and Crowell, R. L. (1995). Receptor proteins on newborn Balb/c mouse brain cells for coxsackievirus B3 are immunologically distinct from those on HeLa cells. *Virus Res.* **35,** 323–340.
40. Wickham, T. J., Mathias, P., Cheresh, D. A., and Nemerow, G. R. (1993). Integrins alpha v beta 3 and alpha v beta 5 promote adenovirus internalization but not virus attachment. *Cell* **73,** 309–319.
41. Roelvink, P. W., Kovesdi, I., and Wickham, T. J. (1996). Comparative analysis of adenovirus fiber–cell interaction: Adenovirus type 2 (Ad2) and Ad9 utilize the same cellular fiber receptor but use different binding strategies for attachment. *J. Virol.* **70,** 7614–7621.
42. Tiemessen, C. T., and Kidd, A. H. (1995). The subgroup F adenoviruses. *J. Gen. Virol.* **76,** 481–497. [Published erratum appears in *J. Gen. Virol.*, 1995, **76,** 2413]
43. Roelvink, P. W., Lizonova, A., Lee, J. G., Li, Y., Bergelson, J. M., Finberg, R. W., Brough, D. E., Kovesdi, I., and Wickham, T. J. (1998). The coxsackievirus–adenovirus receptor protein can function as a cellular attachment protein for adenovirus serotypes from subgroups A, C, D, E, and F. *J. Virol.* **72,** 7909–7915.
44. Leon, R. P., Hedlund, T., Meech, S. J., Li, S., Schaak, J., Hunger, S. P., Duke, R. C., and DeGregori, J. (1998). Adenoviral-mediated gene transfer in lymphocytes. *Proc. Natl. Acad. Sci. USA* **95,** 13159–13164.

Received October 12, 1999
Revised version received October 29, 1999